Journal of Applied Mechanics and Technical Physics, Vol. 40, No. 1, 1999

GAS-DYNAMIC FLOW STRUCTURE OF A SYSTEM OF PLANE SUPERSONIC INTERSECTING JETS IN A HYPERSONIC FLOW

U. K. Zhapbasbaev

UDC 532.526

Turbulent motion is described by a system of parabolized Navier–Stokes equations which is closed by the (k–ε) model of turbulence. In the numerical calculations performed by the method of decomposing the flow vectors, the complex pattern of the interaction between perturbation waves is shown. In addition, it is shown that the system of shock waves on a gas-dynamic site causes the production of the pulsation-motion energy and the appearance of dissipative cellular structures in the field of kinetic turbulence energy.

Introduction. Mixing of fuel jets with the wake of an oxidizer plays an important role in the organization of supersonic hydrogen combustion in the combustion chamber of a hypersonic ramjet. One way to improve the process of mixture formation is to supply supersonic hydrogen jets to a hypersonic air flow at a small angle. The related experimental and calculational-theoretical studies are mainly devoted to the development of supersonic jets in a surging flow [1, 2], whereas data on intersecting jets are lacking. In this connection, the present work deals with a calculational-theoretical study of the system of plane intersecting supersonic jets in a hypersonic flow, and the effect of shock waves on the turbulent flow characteristics, which determine the process of jet–flow mixing, is shown.

1. Physicomathematical Flow Model. We consider the flow in the field of turbulent mixing of a system of supersonic intersecting plane hydrogen jets with a hypersonic air flow (Fig. 1). A jet flows out at a small angle h_1 from flat slits of height $2h_3$ located at the distance α from each other into a hypersonic air flow. The OX axis is directed along the plane of symmetry of the flow, and the OY axis is perpendicular to it. The motion in the entire area is assumed to be stationary and supersonic, and the gas is considered viscous and heat-conducting. Owing to the periodicity and symmetrical character of the flow, the development of one jet in a hypersonic flow is considered. The two-dimensional turbulent motion of a gas mixture is described by the system of parabolized time-averaged Navier–Stokes equations

$$\frac{\partial \mathbf{F}}{\partial x} + \frac{\partial \mathbf{G}}{\partial y} = \frac{\partial \mathbf{S}}{\partial y}, \tag{1.1}$$

where

$$\mathbf{F} = \mathbf{F}[\rho u, \rho u^2 + p, \rho uv, (\rho E + p)u, \rho uC], \quad \mathbf{G} = \mathbf{G}[\rho v, \rho uv, \rho v^2 + p, (\rho E + p)v, \rho vC],$$

$$\mathbf{S} = \mathbf{S}\Big[0, \mu_t \frac{\partial u}{\partial y}, \frac{4}{3}\mu_t \frac{\partial v}{\partial y}, \gamma \frac{\mu_t}{\mathrm{Pr}_t} \frac{\partial e}{\partial y} + \frac{\mu_t}{2} \frac{\partial u^2}{\partial y} + \frac{2}{3}\mu_t \frac{\partial v^2}{\partial y}, \frac{\mu_t}{\mathrm{Sc}_t} \frac{\partial C}{\partial y}\Big].$$

Here u and v are the longitudinal and transverse velocity components, ρ is the density, e is the specific internal energy, C is the hydrogen concentration in the mixture, μ_t is the coefficient of dynamic turbulent viscosity, and Pr_t and Sc_t are the turbulent analogs of the Prandtl and Schmidt numbers, which are equal to 0.9.

The equation of state of a perfect gas is written in the form

$$p = \rho RT, \tag{1.2}$$

Al-Farabi Kazakh National State University, Almaty 480121. Translated from Prikladnaya Mekhanika i Tekhnicheskaya Fizika, Vol. 40, No. 1, pp. 108–114, January–February, 1999. Original article submitted April 10, 1997; revision submitted June 10, 1997.

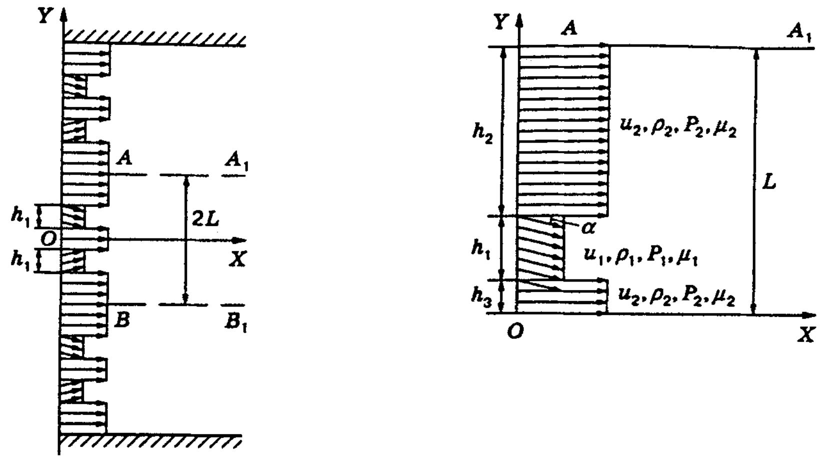

Fig. 1

where $R = R_0 \sum_i C_i/m_i$ (m_i is the molecular mass of the ith component of the mixture and R_0 is the universal gas constant).

The total energy is equal to

$$\rho E = \rho\Big(e + \frac{u^2 + v^2}{2}\Big). \tag{1.3}$$

To calculate the thermophysical properties of a hydrogen–air mixture, the Wilke formula [3] was used. The specific heat of the mixture was found to be $C_V = \sum_i C_i C_{Vi}$. The coefficient of dynamic turbulent viscosity μ_t is determined using the two-parameter (k–ε) model of turbulence [4]:

$$\mu_t = C_\mu \rho \frac{k^2}{\varepsilon}. \tag{1.4}$$

Application of this model in supersonic flows was described by Sinha and Dash [5]. The kinetic turbulence energy k and its dissipation rate ε are found from the equations [4]

$$\begin{aligned} \rho u \frac{\partial k}{\partial x} + \rho v \frac{\partial k}{\partial y} &= \frac{\partial}{\partial y}\Big(\mu_t \frac{\partial k}{\partial y}\Big) + \mu_t \Big(\frac{\partial u}{\partial y}\Big)^2 - \rho\varepsilon, \\ \rho u \frac{\partial \varepsilon}{\partial x} + \rho v \frac{\partial \varepsilon}{\partial y} &= \frac{\partial}{\partial y}\Big(\frac{\mu_t}{\sigma} \frac{\partial \varepsilon}{\partial y}\Big) + C_1 \mu_t \frac{\varepsilon}{k}\Big(\frac{\partial u}{\partial y}\Big)^2 - C_2 \frac{\rho\varepsilon^2}{k}. \end{aligned} \tag{1.5}$$

The constants of the model are as follows: $C_\mu = 0.09$, $C_1 = 1.43$, $C_2 = 1.92$, and $\sigma = 1.3$.

All the parameters which enter into system (1.1)–(1.5) are dimensionless. The coordinates x and y are referred to h_1, the velocity components u and v to U_1, the density ρ to ρ_1, the pressure p to $\rho_1 U_1^2$, the specific internal energy e to U_1^2, the coefficient of turbulent viscosity μ_t to $\rho_1 U_1 h_1$, the kinetic turbulence energy k to U_1^2, and the dissipation rate of the kinetic turbulence energy ε to U_1^3/h_1.

In the initial section, for $x = 0$ the boundary conditions of system (1.1)–(1.5) are of the form

$$u = \frac{\mathrm{M}_2}{\mathrm{M}_1}\sqrt{\frac{R_2 T_2}{R_1 T_1}}, \quad v = 0, \quad \rho = \frac{T_1 R_1}{n T_2 R_2}, \quad e = \frac{C_{V2} T_2}{\mathrm{M}_1^2 T_1 \gamma R_1}, \quad C = 0, \quad k = C_k u^2, \quad \varepsilon = C_\varepsilon \frac{k^{3/2}}{l_\varepsilon}$$

for the flow ($0 \leqslant y \leqslant h_3$ and $1 + h_3 \leqslant y \leqslant L$) and

$$u = \cos\alpha, \quad v = -\sin\alpha, \quad \rho = 1, \quad e = \frac{C_{V1}}{\mathrm{M}_1^2 \gamma R_1}, \quad C = C_0, \quad k = C_k u^2, \quad \varepsilon = C_\varepsilon \frac{k^{3/2}}{l_\varepsilon} \tag{1.6}$$

for the jet ($h_3 < y < h_3 + 1$).

TABLE 1

Condition No.	M_1	M_2	n	T_1, K	T_2, K	C_0	α, deg	h_3	P_{max}/P_1
1	3	10	10	500	500	0.1	3	1	1.08
2	3	10	5	500	500	0.1	3	1	1.15
3	2	6	10	500	500	0.1	12	1	1.30
4	3	10	10	500	500	0.1	12	1	1.50
5	3	10	5	500	500	0.1	12	1	1.56
6	3	10	10	500	500	0.01	12	1	2.12

The symmetry conditions

$$\frac{\partial u}{\partial y} = \frac{\partial \rho}{\partial y} = \frac{\partial e}{\partial y} = \frac{\partial k}{\partial y} = \frac{\partial \varepsilon}{\partial y} = \frac{\partial C}{\partial y} = v = 0 \tag{1.7}$$

are specified on the axis of symmetry $y = 0$ and the upper boundary $y = L$.

Together with the boundary conditions (1.6) and (1.7), system (1.1)–(1.5) is solved by a numerical method. The convective terms and the terms with pressure gradients in the direction of the OX axis are approximated with the left-sided differences owing to the positive eigenvalues of the Jacobi matrix $A = \partial \mathbf{F}/\partial \mathbf{U}$ and with the "counterflow" differences in the direction of the OY axis with allowance for the sign of the eigenvalues of the Jacobi matrix $B = \partial \mathbf{G}/\partial \mathbf{U}$ according to the decomposition scheme of the flow vectors [6]. The terms which describe the viscous shear stresses and the heat flow are approximated by the central differences [7]. As a result, we obtain a difference equation of system (1.1) in the form

$$A_{ij}\Delta \mathbf{U}_{ij} = -\frac{\Delta x}{\Delta y}\left[B^-_{ij+1/2}\mathbf{U}_{ij+1} + B^+_{ij+1/2}\mathbf{U}_{ij} - B^-_{ij-1/2}\mathbf{U}_{ij} - B^+_{ij-1/2}\mathbf{U}_{ij-1}\right]$$
$$+ \frac{\Delta x}{\Delta y^2}\left[\mu_{ij+1/2}(\mathbf{S}_{ij+1} - \mathbf{S}_{ij}) - \mu_{ij-1/2}(\mathbf{S}_{ij} - \mathbf{S}_{ij-1})\right], \tag{1.8}$$

where A and B are the Jacobi matrices of the vectors $\mathbf{F}$ and $\mathbf{G}$, respectively. The values of the matrix B and the coefficient of vortex viscosity μ_t at the half-integer points are determined from the relations

$$B_{ij\pm 1/2} = (1/2)(B_{ij} + B_{ij\pm 1}), \quad \mu_{ij\pm 1/2} = (1/2)(\mu_{ij} + \mu_{ij\pm 1}).$$

The finite-difference equation (1.8) was solved by the Gauss–Seidel method in each section of the marching coordinate x.

The methods of decomposing the flow vectors are physically justified and allow one to trace the perturbation distribution along the characteristic directions. In addition, these methods allow one to obtain solutions with initial discontinuities of the flow parameters and to describe shock waves with steep fronts without the inclusion of artificial dissipative terms [8, 9]. For verification of the numerical method of solution, test calculations were carried out and compared with the calculation according to the characteristics [10] and through-calculation [11] methods. The calculation results show that, just as with the method of characteristics, this scheme of decomposition of the flow vectors traces the perturbation waves and is steady at strong velocity and pressure discontinuities in the initial section of the flow [12].

2. Discussion of Calculation Results. The basic mode parameters of the flow (the degree of noncalculation is $n = p_1/p_2$, the Mach numbers of the jet M_1 and of the flow M_2, the hydrogen concentration in the jet C_0, the jet T_1 and flow T_2 temperatures, and the angle of jet outflow α) are listed in Table 1. The refined fields of pressure, density, temperature, velocities, concentration, and kinetic turbulence energy and the dissipation rates were calculated.

Figure 2 shows the calculation results obtained for the interaction of a supersonic hydrogen jet with a hypersonic air flow [isobars (a) and isotherms (b)] for the following mode parameters: $M_1 = 3$, $M_2 = 10$, $n = 10$, $T_1 = T_2 = 500$ K, and $\alpha = 12°$. The hydrogen concentration in the jet is $C_0 = 0.01$. The larger portion of the mixture is considered passive, i.e., it reacts neither with the fuel (hydrogen) nor with the oxidizer (air). For $h_3 = h_1$ and $\alpha = 12°$, the intersecting jets approach each other and this results in the deceleration of the

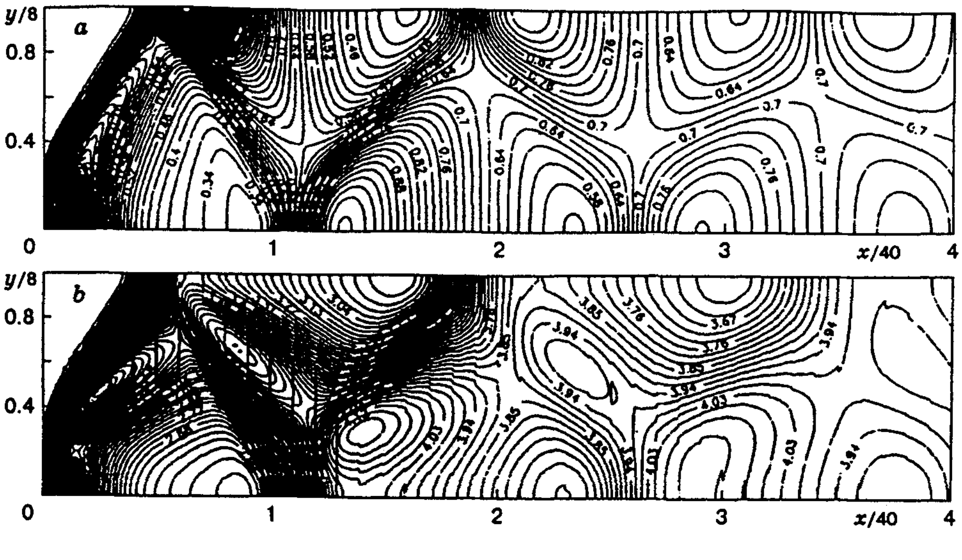

Fig. 2

hypersonic flow located between them. Then, a merged supersonic jet is formed at a distance of three sizes of the jet width. The characteristics in the new jet are distributed nonuniformly and this jet also has a region of higher statistical pressure $p/p_1 \approx 1.6$ which exceeds the initial degree of noncalculation (Fig. 2a). In this zone, the temperature rises to $T/T_1 \approx 4.0$, which is probably caused by the interaction of two intersecting underexpanded jets with the hypersonic flow (Fig. 2b). The Mach number on the line $y = 0$ to this cross section decreases by a factor of more than 2 ($M \approx 4.6$), although the value of the velocity u varies insignificantly. The merged jet begins to expand, the pressure in the central part decreases, and the Mach number is slightly increased. The resulting shock waves attached to the cross section $x \approx 19$ reach the lines of symmetry in the wake $y = L$, where a zone of raised pressure $p/p_1 \approx 2.12$ is formed. In turn, this zone is a source of perturbation waves and a shock wave arriving at the axial plane at a distance of $x \approx 44$. The subsequent development of the flow occurs similarly to that described above. Thus, a system of chess-ordered compression and rarefaction zones appears. These zones have a complex pattern of perturbation waves whose intensity decreases downstream because of the viscous interaction.

The isotherms in Fig. 2b indicate the temperature rise in the shock waves, which exceeds the initial temperature of the jet because of kinetic-energy dissipation by a factor of more than 4.

The distinguishing feature of the intersecting supersonic jets in a hypersonic flow is the increase in pressure, which is caused by deceleration of the flow during interaction with the jet. Table 1 lists the maximum pressure values in the compression zones for various mode parameters. The maximum pressure is most affected by the angle of jet outflow and the hydrogen concentration.

The pattern of variation in the kinetic turbulence energy and the longitudinal velocity component was determined via calculations (Fig. 3, the initial conditions correspond to Fig. 2). As one can see in Fig. 3a, the shock waves emanating from the nozzle edge cause an intense generation of the kinetic turbulence energy k in the initial cross sections of the flow. In the rarefaction field, the kinetic turbulence energy is suppressed. The system of chess-ordered compression and rarefaction zones and the shock waves which separate these zones cause the occurrence of dissipative cellular structures in the field of kinetic turbulence energy k, which can be explained as follows. As mentioned above, a raised-pressure zone, i.e., the source of perturbation waves, is formed at the site where the attached shock wave is reached at the flow boundary ($x \approx 19$). The shock wave outgoing from this zone leads to an abrupt change in the parameters of the averaged motion (the velocity, pressure, temperature, and density) and causes the generation of the kinetic turbulence energy. The same change occurs behind the shock wave reflected from the plane of symmetry; note that the flow decelerates before the shock wave and accelerates behind it. This is well illustrated by the isotherms of the longitudinal

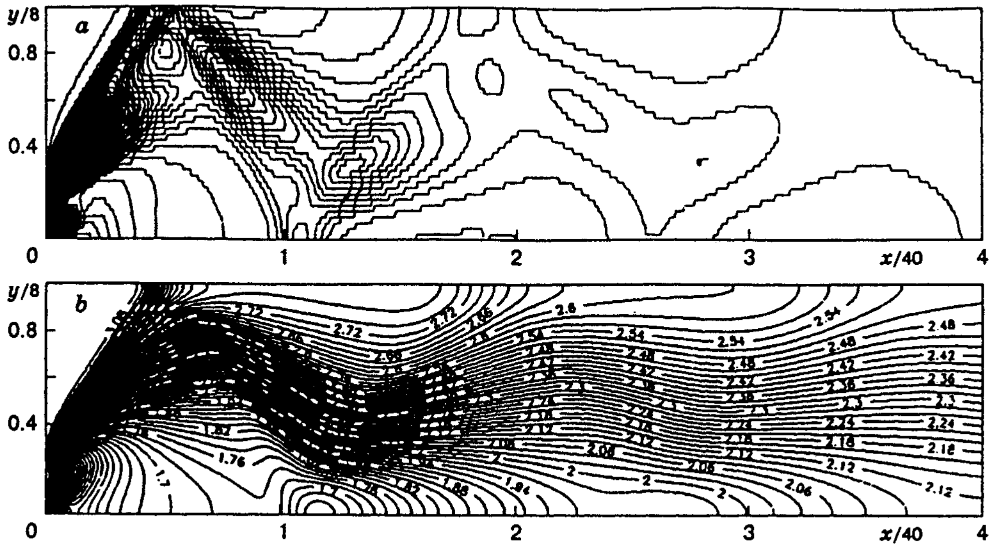

Fig. 3

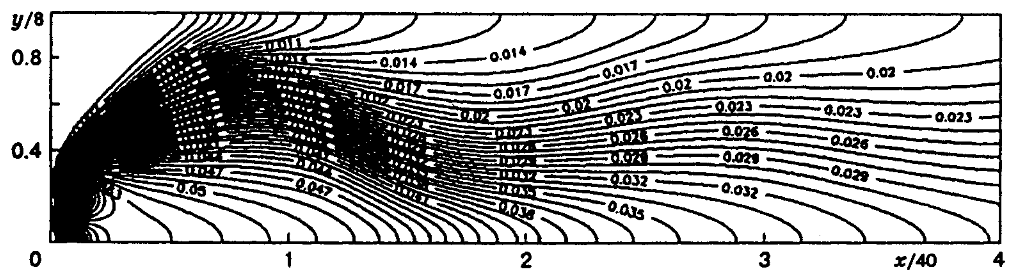

Fig. 4

velocity component (Fig. 3b). The cellular structures, which reflect the increase in the kinetic turbulence energies on shocks, dissipate in the region of flow expansion (Fig. 3a). The following pair of shock waves again leads to the production of kinetic turbulence energy. Downstream, as the perturbation and shock-wave power decrease, the intensity of the dissipative structures in the field of kinetic turbulence energy decreases. Thus, affecting the averaged-motion parameters, the system of shock waves in the gas-dynamic section of the flow leads to the appearance of dissipative cellular structures in the field of kinetic turbulence energy.

The hydrogen-concentration isolines in Fig. 4 illustrate the mixing pattern of the intersecting supersonic jets in a hypersonic flow under condition No. 1 (see Table 1). It is seen that almost 50% of hydrogen is mixed with air at the site of confluence of the intersecting jets, and the other portion of hydrogen in the merged jet scatters in the hypersonic flow. The variation in the angle α in the range of $3^\circ \leqslant \alpha \leqslant 12^\circ$ does not exert, with other things being equal, a significant effect on the mixing of plane supersonic intersecting hydrogen jets with a hypersonic air flow.

The results allow us to draw the following conclusions:

1. The interaction of a system of intersecting supersonic jets with a hypersonic flow leads to a complex pattern of the compression and rarefaction zones; note that the static pressure in the compression zones exceeds the initial degree of noncalculation of the flow and is a source of propagation of perturbation waves.

2. The system of shock waves in the gas-dynamic section of the flow causes the production of pulsation-motion energy and the appearance of dissipative cellular structures in the field of kinetic turbulence energy. The configuration of these dissipative structures is determined by the location of shock waves and the wave character of the static-pressure distribution.

REFERENCES

1. J. A. Schetz, *Injection and Mixing in Turbulent Flow*, New York Univ., New York (1980).
2. V. S. Avduevskii, É. A. Ashratov, A. V. Ivanov, and U. G. Pirumov, *Gas Dynamics of Supersonic Nonisobaric Jets* [in Russian], Mashinostroenie, Moscow (1989).
3. R. C. Reid, J. M. Prausnutz, and T. Sherwood, *The Properties of Gases and Liquids*, McGraw-Hill, New York (1977).
4. B. Launder, A. Morse, W. Rodi, and D. B. Spalding, *Prediction of Free Shear Flows — A Comparison of the Performance of Six Turbulence Models*, New York (1971). (NASA SP-321).
5. N. Sinha and S. M. Dash, "Parabolized Navier–Stokes analysis of ducted turbulent mixing problems with finite rate chemistry," AIAA Paper No. 86-0004, New York (1986).
6. J. L. Steger and R. F. Warming, "Flux vector splitting of the inviscid gas dynamics equations with application to finite difference methods," *J. Comput. Phys.*, **40**, 263–293 (1981).
7. J. L. Thomas and R. U. Walters, "Relaxation schemes with counterflow differences for Navier–Stokes equations," *Aerokosm. Tekh.*, No. 2, 13–23 (1988).
8. T. Y. Coakley, "Implicit upwind methods for the compressible Navier–Stokes equations," *AIAA J.*, **23**, No. 3, 374–384 (1985).
9. J. Marvin and T. Y. Coakley, *Turbulence Modeling for Hypersonic Flows*, New York (1989). (NASA TM-101079).
10. G. I. Averenkova, É. A. Ashratov, T. G. Volkonskaya, et al., *Supersonic Jets of Ideal Gas* [in Russian], Part 1, Comput. Center of the Moscow State University, Moscow (1970).
11. M. Ya. Ivanov and A. N. Kraiko, "Numerical solution of the problem of noncalculated outflow of the supersonic jet of a viscous gas into a supersonic wake," in: *Numerical Methods of Continuum Mechanics* (collected scientific papers) [in Russian], Vol. 6, No. 2, Inst. of Theor. and Appl. Mech., Sib. Div., Acad. of Sci. of the USSR (1975), pp. 37–47.
12. U. M. Sultangazin, A. Sh. Ershina, and U. K. Zhapbasbaev, "Wave structure in a calculated regime of outflow of a system of plane supersonic wake jets," *Vestn. Akad. Nauk Kaz. SSR*, No. 11, 50–56 (1990).